Electronic Supplementary Material (ESI) for Lab on a Chip

Dielectrophoretic Tweezers as a Platform for Molecular Force Spectroscopy in a Highly Parallel Format

Peng Cheng, Michael J. Barrett, Piercen M. Oliver, Deniz Cetin, Dmitri Vezenov*

Lehigh University, Department of Chemistry, 6 E. Packer Ave., Bethlehem, PA, 18015, USA
E-mail: dvezenov@lehigh.edu

Supplementary Information

S1. Parameters for numerical simulations

In 3D calculations (Figure S1), the number of degrees of freedom is dramatically greater than in 2D calculations; therefore, an optimal choice of the proper mesh size is critical to reduce computation time.

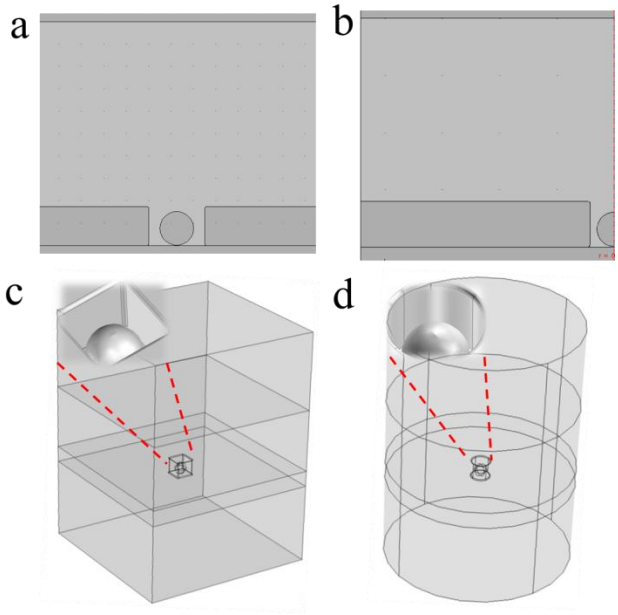

Figure S1. Geometry of simulations for a square well in full 3D (a, c) and a round well in reduced 3D (b, c) simulations.

We investigated the sensitivity of the numerical results to different mesh sizes. The size and the height of the wells, the separation between two electrodes and the diameter of the probes have the same values as the standard parameters mentioned in the main text. The probes were set at 50 nm above the bottom of the well. The DEP forces obtained by both EDA and MST methods converged to constant values when the mesh size was smaller than 25 nm (Figure S2). We then kept 25 nm as a meshing parameter in the following calculations.

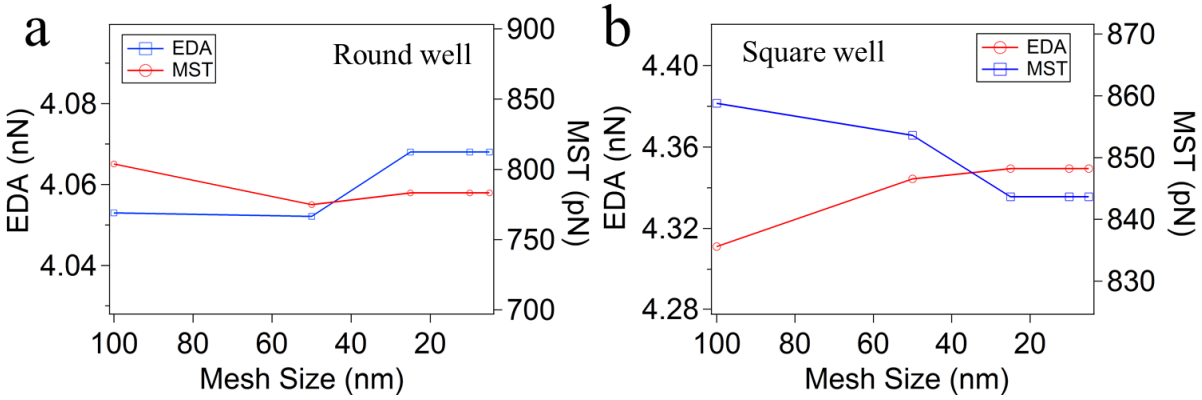

Figure S2. DEP forces for beads in Geometry C calculated using EDA and MST methods are plotted versus the mesh sizes for 3D simulation with a round well (a) and square well (b).The potential was set to 10 V (peak to peak).

EDA model (Equation 1 in the main text of the paper) considers the probe as a single dipole. This approximation is normally sufficient for cases where the electric field does not change appreciably over distances comparable to probe size. We verified the results obtained using the EDA model by carrying out rigorous MST calculations on the same systems. Figure S3 represents the results of the calculations of the DEP force in the setups shown in Figure S1 above.

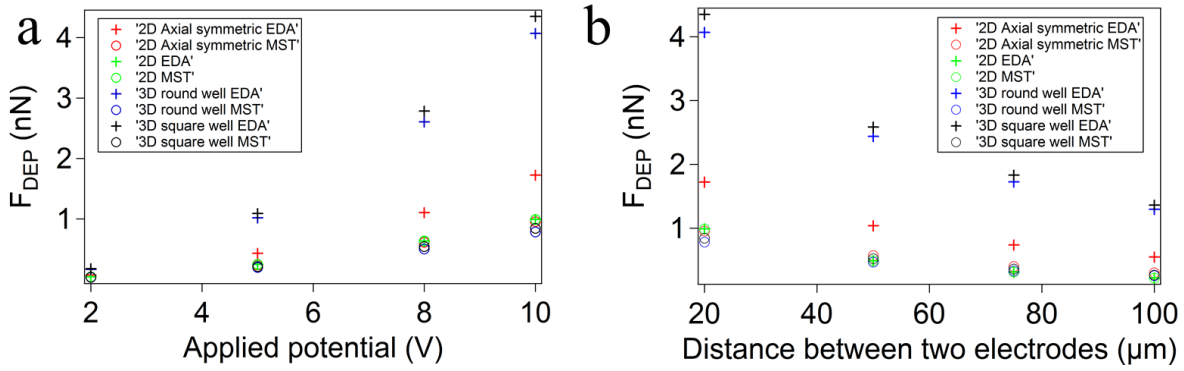

Figure S3. Both of EDA and MST methods are used for calculation of the DEP force. (a) The DEP force varies as a function of applied potential while the electrode separation was set at 20 μm. (b) Change in the DEP force with respect to the distance between two electrodes while the applied potential was set at 10 V.

Two parameters were varied in those calculations. When the applied potential between two electrodes increases, DEP force exerted on the probe increases (Figure S3a). When the distance between two electrodes increases, DEP force diminishes (Figure S3b). Forces calculated using MST-based approach cluster very tightly and show self-consistency between all models. However, the EDA results span a wide range of DEP force values for the same geometry and set of parameters (could differ by > a factor of 4), indicating that EDA is only a first order approximation that will overestimated the DEP force for all 3D models. Only the 2D model produced similar results for DEP forces with both EDA and MST methods. We can conclude that 2D simulation for force calculations using MST integration is the optimum approach to balance requirements on the computation time with the accuracy when simulating various DEP tweezers designs.

S2. Microfabricated substrates suitable for TIRF microscopy of probes

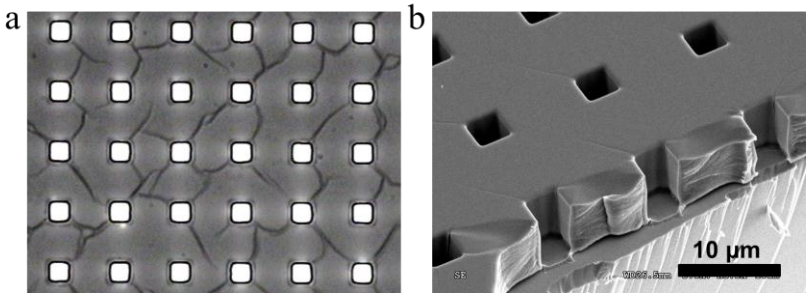

Figure S4. (a) A transmission light microscopy image of the microwell substrate suitable for TIRF microscopy. (b)) A typical SEM image of the patterned bottom electrode.

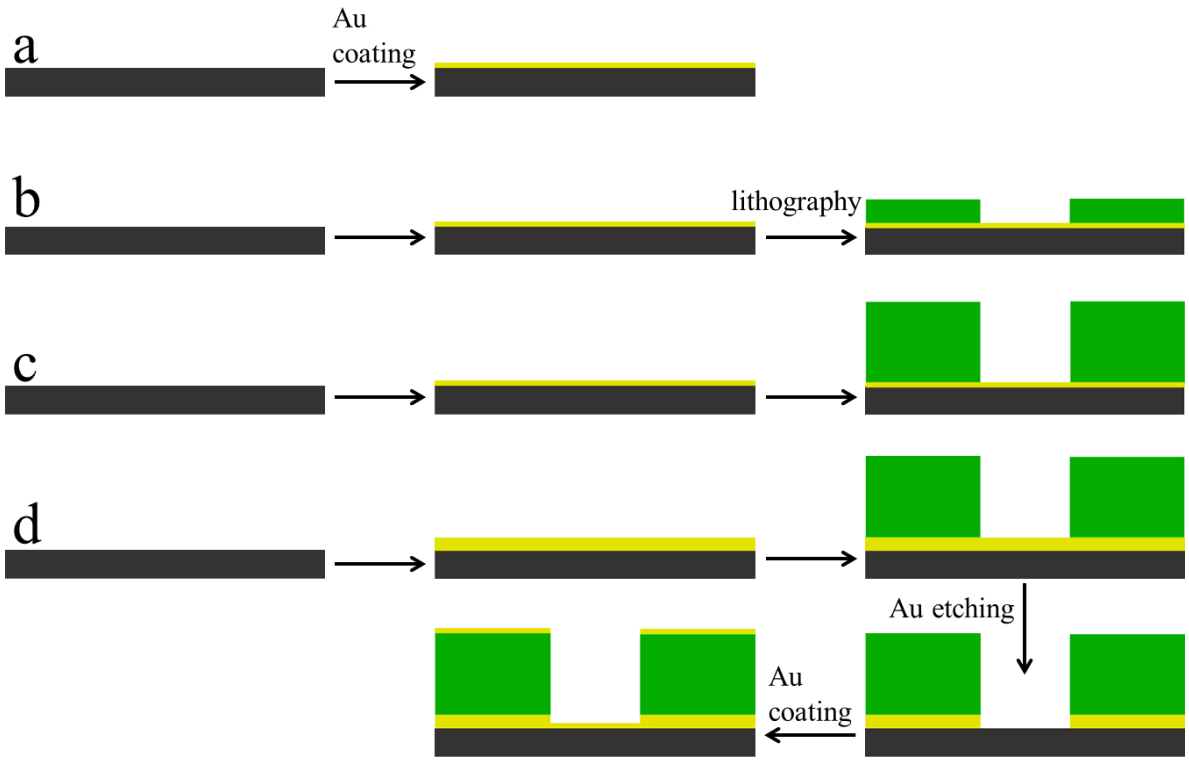

Figure S5. Fabrication scheme for all four designs. (a) Top-plate and geometry A were fabricated by coat thin metal layer (4.5 nm Titanium and 11 nm gold) on different size cover glass. (b) and (c) Fabrication of design B and C was integrating different height wells on design A by photo-lithography. (d) For the TIRF suitable substrates, we did a thick metal layer (4.5 nm Titanium and 130 nm gold) on the cover glass and followed by micro-fabricating micro-wells on the surface of those substrates. We then etched the gold in the bottom of the well. For the final step, we coated a metal layer (4.5 nm Titanium and 11 nm gold) for gold-thiol chemistry.

In order to prevent the light from propagating in the SU-8 layer, which will result in illumination of the probes in an unpredictable fashion, we fabricated substrates that blocked the light from entering the SU-8 layer at the glass/SU-8 interface. We first deposited a 130 nm gold film on the glass cover slips. After the lithographic fabrication of the micro-well structure, we applied a standard gold etchant (4 g KI, 1 g I_2, and 80 mL DI-H_2O) to remove gold film from the bottom of the wells. The formation of the transparent wells is readily confirmed by transmission light microscopy. The light is blocked from the area around the well by the thick gold film (Figure S4). A 15 nm semi-transparent gold film was then deposited onto the substrate resulting in Geometry D DEP cell (see Figure 2d in the main text).

S3. Fluorescent colloidal probes

The probes were fabricated by membrane emulsification of PMMA-PAA (100:1) co-polymer (MW~30kDa) and characterized using scanning electron microscopy (Hitachi 4300 SEM). The diameter of the probes had a width of distribution (standard deviation) of approximately 10% of the mean. The zeta potential measurements indicated presence of the COOH groups on the surface as evidenced by transition from 0 mV (pH<5) to 30 mV(pH>5).

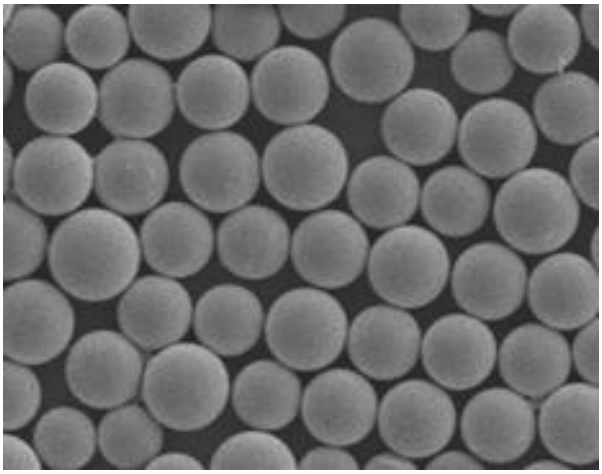

Figure S6. SEM image of the polymer probes fabricated by membrane emulsification method.

S5. Voltage dependence of the DEP force on probes in microwells

We calculated the changes in the DEP force generated on a flat electrode and in a 4 μm height micro-well (Geometry C) when voltage between two electrodes was varied. The DEP force exerted on the probe follows a power law and the fitted value for an exponent is exactly 2 (as in the flat electrodes case for Geometry A).

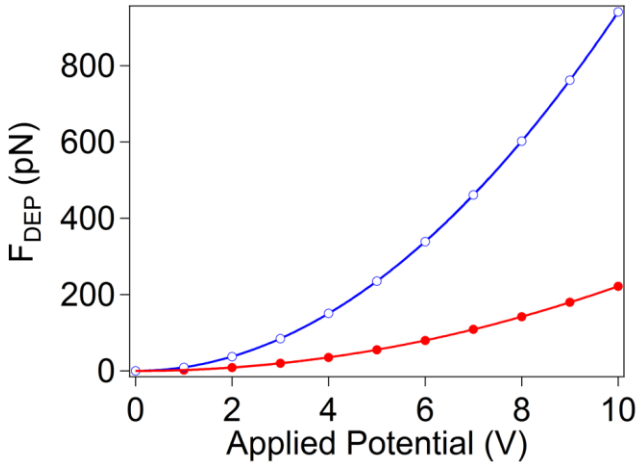

Figure S5. Simulation results of DEP force acting on a probe which is 50 nm away from the surface as a function of potential applied between two parallel electrodes separated by 24.5 μm for Geometry A (●) and C (○). For Geometry A, the line is a power law fit $F_{DEP}=2.22V^{2.00}$ (where F is in piconewtons, V is volts, standard deviation for both coefficients is < 0.003%). For Geometry C, the line is a power law fit $F_{DEP}=9.41V^{2.00}$ (where F is in piconewtons, V is volts, standard deviation for both coefficients is < 0.003%).

S6. Derivation of DEP force as a function of electrode separation

For Geometry C, there are two layers with different dielectric constants in the capacitor. The total potential is:

$$V = E_{water} \cdot (S - h) + E_{resist} \cdot h$$

$$V = \frac{E_0}{\varepsilon_{water}} \cdot (S - h) + \frac{E_0}{\varepsilon_{resist}} \cdot h$$

$$E_0 = \frac{q}{\varepsilon_0 \cdot A}$$

where q is the total charges on the electrode, ε_0 is the vacuum permittivity, and A is the area of the two electrodes.

The electric field in the photoresist should be:

$$E_{resist} = \frac{E_0}{\varepsilon_{resist}} = \frac{V}{s\,\frac{\varepsilon_{resist}}{\varepsilon_m} + h\left(1 + \frac{\varepsilon_{resist}}{\varepsilon_m}\right)}$$

S7. Normal forces for Geometry D

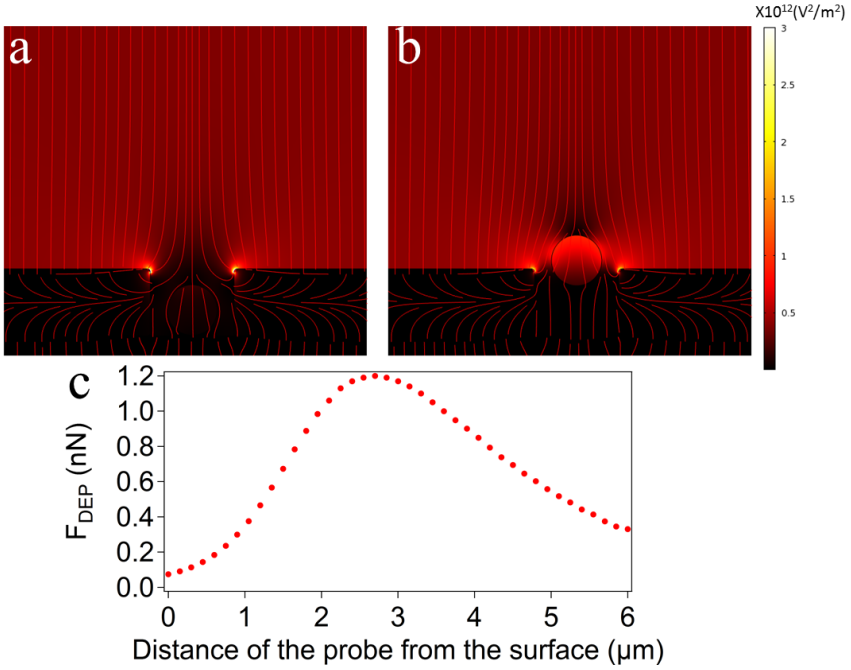

Figure S8. Electric field distributions in Geometry D for a 3 μm diameter probe at 50 nm (a) and 3 μm (b) above the surface of the electrode. The probe is pulled up (F_{DEP}>0) by the positive DEP force in (a) and (b). The red streamlines represent the electric field. The surface plots are $\boldsymbol{E^2}$ and two graphs share the same scale. (c) The DEP forces versus distance from the surface when the 3 μm probe is moving away from the electrode. The DEP force linearly increases when the probe moves from contact to 500 nm away from the surface of the electrode.

S8. Electric field distribution inside a round well in Geometry D.

We simulated electric field distribution from the incident laser beam inside microwells using numerical code we developed for numerical analysis of the bead fluorescence excited by the evanescent wave (A. Bijamov, F. Shubitidze, P. M. Oliver and D. V. Vezenov, *Langmuir*, **2010**, *26*, 12003-12011). The presence of a dielectric with high dielectric permittivity in contact with glass breaks the condition for the total internal reflection of the waves incident from the glass coverslip. Although the TIR condition still holds at the glass-water interface, the propagating waves that originate at the glass-dielectric boundary can make their way inside the well and overwhelm the evanescent waves produced due to the total internal reflection. A thin layer of metal (~100 nm of gold) placed between glass and photoresists pattern is sufficient to block the propagation of waves into SU-8, preventing them from entering the well. The evanescent wave is then confined to a thin layer of water in the vicinity of the glass and its intensity decays towards the sidewalls. Due to the reflection from the walls of the well, an interference pattern develops inside the well, although its effect is likely to be minor due to more than an order of magnitude drop in intensity in the region where the variation in intensity becomes pronounced.

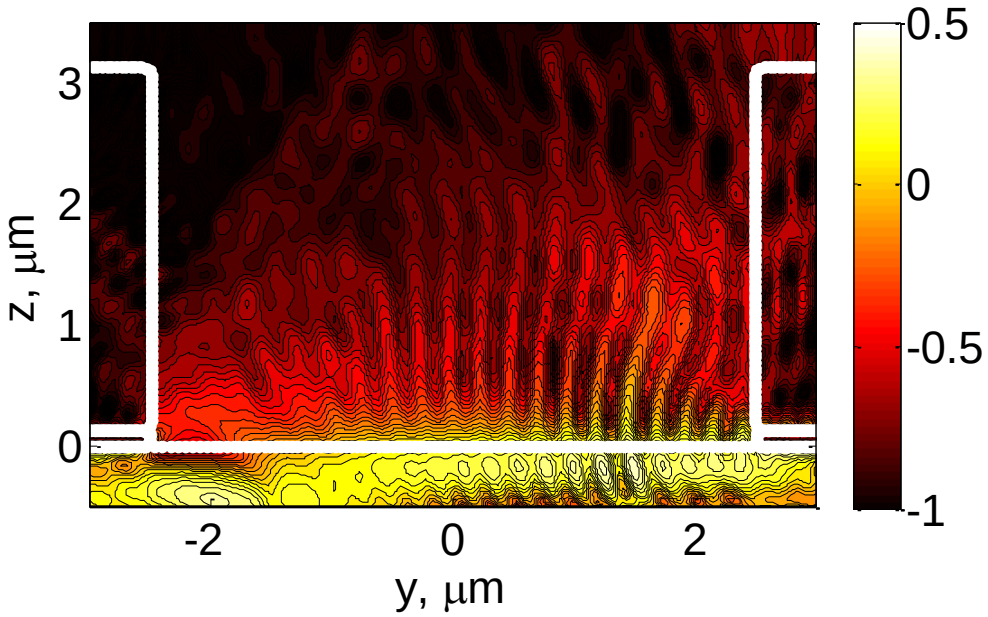

Figure S9: Electric field intensity distribution ($\log_{10}$ scale) inside a well.

Acknowledgement

We thank Dr. Alex Bijamov (Dartmouth College) for performing the simulation shown in Figure S9.